RESEARCH ARTICLE

Analysis of change process of NPP dominated by human activities in Northwest Hubei, China, from 2000 to 2020

Shuai Shao[1] · Yong Yang[1]

Abstract

Clarifying the spatial distribution of the impact of different human disturbance activities on the net primary productivity (NPP) in regions with single climatic conditions is of considerable importance to ecological protection. Time-series NPP from 2000 to 2020 was simulated in Northwest Hubei, China, and the effects of the climate and human activities on the NPP changes were separated. Research results showed that from 2000 to 2020, the NPP change with an area of 10,166.63 km^2 in Northwest Hubei is influenced by climate and human activities. Among them, human activities account for as high as 84.53%. From 2000 to 2020, the NPP in Northwest Hubei showed a slight upward trend at a rate of 1.61 g C m^{-2} year^{-1}. The significantly increased NPP accounted for 21.4% of the total, which was mainly distributed in north of Northwest Hubei. And the farming of cultivated land led to the increase of NPP in west as well as the reduced human distribution in cultivated land, which was scattered in forests. Only 6.67% of the total area demonstrated a significantly decreased NPP, which was distributed mainly in the central affected by the expansion of rural–urban land and change of broad-leaved forests to shrubs and in southeast regions of Northwest Hubei caused by the increase in potential evapotranspiration. This study refined the driving factors of spatial heterogeneity of NPP changes in Northwest Hubei, which is conducive to rational planning of terrestrial ecosystem protection measures.

Keywords Net primary productivity · Climate change · Human interference degree · Dynamic change · Influence mechanism · Northwest Hubei

Introduction

Vegetation is the primary producer of terrestrial ecosystems, which can potentially offset one third of the total fossil fuel emissions (Friedlingstein et al. 2019; Le Quere et al. 2018). Net primary productivity (NPP) is widely used to examine the carbon balance of terrestrial ecosystems (Bai et al. 2023; Hsu et al. 2012; Zhuang et al. 2022). However, climate change and human activities dramatically altered the structure, functions, and services of terrestrial ecosystems (Izaurralde et al. 2005; Stevens-Rumann et al. 2018; Xiao

et al. 2023). Therefore, quantifying the main drivers of spatiotemporal changes in NPP is of considerable importance to regional vegetation to maintain ecosystem stability.

Numerous quantitative studies assessed the spatiotemporal changes in NPP around the world (Koju et al. 2020; Nayak et al. 2013). However, the potential separate or common impacts of climate change and human activities on vegetation remain uncertain, especially at the regional scale. Therefore, separating the impact of climate change and human activities on vegetation is crucial (Chen et al. 2019; Dariane and Pouryafar 2021). Unaltered natural vegetation affected only by climate change and vegetation affected by climate change and human activities were separated using multitemporal land use/land cover data (Ge et al. 2021). Teng et al. (2020) separated NPP influenced by human activities by estimating the difference between the actual NPP calculated with the Carnegie-Ames-Stanford approach (CASA) and NPP influenced by the climate based on evapotranspiration, precipitation, and temperature. Zhang et al. (2021) disentangled the effects

✉ Yong Yang
yangyong@mail.hzau.edu.cn

Shuai Shao
ss1603759331@outlook.com

1 College of Resources and Environment, Huazhong Agricultural University, Wuhan 430070, China

of land cover change and climate change on gross primary production according to the scenario setting. For example, to separate the impact of land cover change on gross primary productivity (GPP), the authors set the land cover to the initial period level but allowed all the other variables to change. Li et al. (2021) used the fraction of absorbed photosynthetically active radiation (FPAR) estimated by the leaf area index to separate the impact of climate change on NPP. Most of the above studies employed empirical models to separate the effects of the climate and human activities on changes in the NPP. In addition, many studies focused on the use of statistical methods to distinguish the effects of the climate and human activities on vegetation. According to the residual trend method, Qi et al. (2019) determined the relative effects of the climate and human activities on vegetation over multiple timescales in China's Silk Road Economic Belt. Wu et al. (2020) analyzed the impact of climate change and human activities on changes in vegetation productivity based on NPP using the partial correlation in karst areas in China.

The dynamic effects of the climate and human activities on vegetation demonstrate obvious spatial heterogeneity. In arid and semiarid regions, the grassland carbon sequestration process is highly susceptible to climate change, especially precipitation (Wang et al. 2019). From 1982 to 2008, increased vegetation greenness was observed in 27% of the protected areas monitored in Africa (mostly in West Africa), and the changes in the NPP dynamics coincided with the changes in precipitation (Pettorelli et al. 2012). In Central Asia, temperature and precipitation have significant effects on vegetation phenology and NPP owing to the stress induced by drought conditions (Wu et al. 2021). Temperature was highlighted as the main driver of the NPP projections for the Antarctic tundra biome, which showed that climate warming will lead to an average increase in the NPP of 167–171% at the end of the century (Beltrán-Sanz et al. 2022). The above studies are concentrated mainly in ecologically sensitive areas, where the vegetation is significantly affected by climate change. Existing research also showed that the human appropriation of the NPP can significantly alter the energy flow of ecosystems (Haberl 1997). The artificial disturbance of the potential natural NPP state of the occupied land may exert significant pressure on the biodiversity (Haberl et al. 2005). At the same time, countries and regions engaged in considerable ecological restoration work to improve the ecological environment (Liu et al. 2019; Yang et al. 2014; Zhang et al. 2020). The above studies mostly analyzed the influence factors of climate change and human activities on the changes in the NPP on a large scale. However, there are significant differences in the impact of climate change and human activities on ecosystem services at different scales (Bejagam and Sharma 2022). Therefore, this study attempts to explore the spatial distribution characteristics of

the impact of different driving factors on NPP at the regional scale.

In addition, to examine the impact of climate change and human activities on NPP changes, previous studies mostly adopted the absolute amount of change and often ignored the ecological process (Li and He 2022; Yang et al. 2021). Therefore, this study explores the spatial heterogeneity of the impact of the climate and human activities on vegetation based on the spatiotemporal variation characteristics of time-series NPP. This research aims to (1) simulate the annual NPP in Northwest Hubei (Exibei, in this study) from 2000 to 2020 with the CASA and analyze its variation trend and (2) determine the main driving factors of the interannual spatiotemporal variation in the regional NPP.

Materials and methods

Study area

Exibei (109°29′E–113°6′E, 31°14′N–33°17′N) is located in Northwest Hubei Province and covers an area of 46,660 km^2 (accounting for 25% of the total area of Hubei Province). The elevation of the study area is within the range of 33–3097 m, showing a descent from south to west. Exibei is surrounded by mountains on three sides, with abundant mountain resources. It borders the Qinling Mountains to the north, Bashan Mountains to the south, and Wushan Mountains to the west. The western region of the study area is mountainous (mainly covered by evergreen broad-leaved forest, deciduous broad-leaved forest, and evergreen needle-leaved forest), and the eastern region is plain. Therefore, Exibei has become an important component of the ecological barrier in the Qinba Mountains. In addition, there are numerous rivers and lakes in northwest Hubei, which provide excellent soil and water conditions for the eastern plain and supporting it as the main grain-producing area of the country. In terms of climate, Exibei belongs to the north subtropical humid region, characterized by hot and rainy summers and mild and rainy winters. The average annual precipitation is between 800 and 1000 mm, and the average annual temperature ranges from 15 to 18 °C.

Data description

The land cover data from 2000 to 2020 were obtained from the European Space Agency Climate Change Initiative. In this study, the land cover types were reclassified into nine categories, which are shown in Fig. 1. The MODIS Normalized Difference Vegetation Index (NDVI) with 16-day 250-m spatiotemporal resolution was provided by the National Aeronautics and Space Administration (https://lpdaacsvc.cr.usgs.gov/appeears/). Subsequently, the monthly NDVI was obtained

Fig. 1 Location of study area
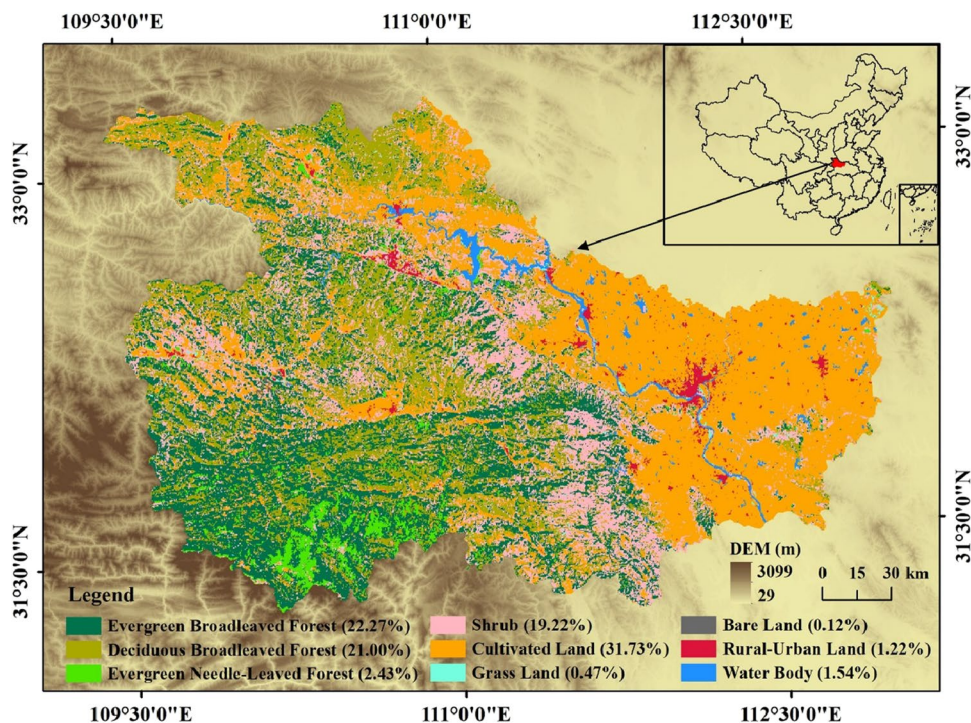
by Savitzky–Golay filtering according to the detailed quality assess (QA) band and then maximum synthesis. The meteorological data included precipitation, annual average temperature, solar radiation, and potential evapotranspiration. The data on precipitation, annual average temperature, and potential evapotranspiration were obtained from the National Earth System Science Data Center (http://www.geodata.cn/), and the information on solar radiation was obtained from ECMWF Reanalysis v5 (ERA5) (https://cds.climate.copernicus.eu/). The spatial resolution of all the data was resampled at 250 m.

Methodology

NPP estimation

NPP, as the basis for the study of material and energy transport in terrestrial ecosystems, is an ideal indicator for characterizing the carbon sequestration capacity of vegetation in regional ecosystem functions. It is the net accumulation of organic matter in photosynthesis by vegetation after subtracting its own respiration consumption. The time-series NPP was simulated with the CASA, which is a process-based model driven by remote sensing and climate data (Field et al. 1995; Potter et al. 1993). The NPP was determined mainly by two variables: absorbed photosynthetic active radiation (APAR) and light energy utilization ratio (ε):

$$NPP(x,t) = APAR(x,t) \times \varepsilon(x,t)()$$ (1)

where $NPP(x,t)$ (g C m^{-2} year^{-1}) is the vegetation NPP at time t in pixel x. $APAR(x,t)$ (MJ m^{-2}) and (x,t) (g C MJ^{-1}) are the photosynthetic effective radiation absorbed by the pixel x at time t, and the actual light energy utilization of the pixel x at time t, respectively.

$$APAR(x,t) = SOL(x,t) \times FPAR(x,t) \times 0.5()$$ (2)

where $SOL(x,t)$ (MJ m^{-2}) represents the total solar radiation, the constant 0.5 represents the proportion of the total solar radiation that can be effectively utilized by the vegetation, and $FPAR(x,t)$ represents the fraction of the photosynthetically active radiation absorbed by the vegetation, which can be estimated by the NDVI and simple ratio (SR) index of the different vegetation types.

Within a certain range, a linear relationship exists between the FPAR and NDVI and SR index (Field et al. 1995; Ruimy et al. 1994). Therefore, to minimize the estimation error, Los (1998) combined the two methods and took the average as the FPAR estimate:

$$FPAR(x,t) = \frac{(NDVI_{(x,t)} - NDVI_{(i,min)})}{(NDVI_{(i,max)} - NDVI_{(i,min)})} \left(FPAR_{max} - FPAR_{min} \right) + FPAR_{min}()$$ (3)

$$FPAR(x,t) = \frac{(SR_{(x,t)} - SR_{(i,min)})}{(SR_{(i,max)} - SR_{(i,min)})} \left(FPAR_{max} - FPAR_{min} \right) + FPAR_{min}()$$ (4)

$$SR(x,t) = \frac{1 + NDVI_{(x,t)}}{1 - NDVI_{(x,t)}}()$$ (5)

$$FPAR_{(x,t)} = \frac{FPAR_{(NDVI)} + FPAR_{(SR)}}{2}() \tag{6}$$

where $NDVI_{(i,max)}$ and $NDVI_{(i,min)}$ correspond to the maximum and minimum value of the NDVI of the i th vegetation type, respectively; $SR_{(i,max)}$ and $SR_{(i,min)}$ correspond to the $NDVI_{(i,max)}$ and $NDVI_{(i,min)}$ of the i th vegetation type, respectively; and the value of $FPAR_{max}$ and $FPAR_{min}$ is unconcerned with the vegetation type, which is 0.95 and 0.001, respectively.

In an ideal natural environment, the maximum value of the light use efficiency of vegetation can be obtained, but in an actual environment, it is constrained by the temperature and soil moisture conditions:

$$\varepsilon(x,t) = T_{\varepsilon1}(x,t) \times T_{\varepsilon2}(x,t) \times W_{\varepsilon}(x,t) \times \varepsilon_{max}() \tag{7}$$

where $T_{\varepsilon1}(x,t)$ and $T_{\varepsilon2}(x,t)$ represent the stress effect on light use efficiency at low and high temperatures, respectively; $W_{\varepsilon}(x,t)$ is the moisture stress condition, which reflects the reduction in the light use efficiency caused by the moisture factor, and ε_{max} is a set of parameters that represents the maximum light use efficiency under ideal conditions for various vegetation types.

HID

In this study, the human interference degree (HID) was used to express the impact of human activities. Land cover change is the most direct manifestation of the impact of human activities. Human disturbances that cause different land use/cover patterns and intensities have regional and cumulative characteristics. First, in this study, the evaluation unit was determined as 1 km * 1 km, and each obtained HID value was used as the center point value of the evaluation unit. Kriging interpolation was performed to generate the spatial distribution map of the HID in Exibei for each year:

$$HID = \sum_{i=1}^{n} f_i \times h_i,() \tag{8}$$

where n is the number of land cover types, h_i is the disturbance intensity of the i th land cover type, and f_i is the area proportion of the i th land cover type in the evaluation unit. The h_i of the evergreen broad-leaved forest, shrubs, bare land, deciduous broad-leaved forest, cultivated land, rural–urban land, evergreen needle-leaved forest, grassland, and water body is 2, 3, 1, 2, 5, 6, 2, 4, and 2, respectively.

Trend analysis

The combination of Theil–Sen median trend analysis (Sokal 1982) and the Mann–Kendall (MK) test (Kendall 1938; Mann 1945) has become a mature method for the long-term series analysis of vegetation. Compared with linear regression

analysis, this method has the advantages of not requiring the data samples to follow a specific distribution, being less susceptible to outlier interference, and having a strong ability to avoid measurement errors or abnormal data:

$$\beta = Median\left(\frac{x_j - x_i}{j - i}\right), \forall i < j() \tag{9}$$

where β is the vegetation change trend; i and j are the time series; x_i and x_j represent the vegetation at times i and j, respectively; $\beta > 0$ reflects the increasing vegetation trend; $\beta < 0$ reflects the decreasing trend of the NDVI; and $\beta = 0$ reflects no vegetation trend change.

The MK test was used to judge the trend significance, which is defined as follows: for a series of $X_t = (x_1, x_2, \ldots, x_n)$, the Z statistic used for the trend test is calculated as follows:

$$Z = \begin{cases} \frac{S-1}{\sqrt{var(S)}}, & S > 0 \\ 0, & S > 0 \\ \frac{S+1}{\sqrt{var(S)}}, & S < 0 \end{cases}() \tag{10}$$

$$S = \sum_{i=1}^{n-1} \sum_{j=i+1}^{n} sgn(x_j - x_i)() \tag{11}$$

$$sgn(\theta) = \begin{cases} 1, & \theta > 0 \\ 0, & \theta = 0 \\ -1, & \theta < 0 \end{cases}() \tag{12}$$

$$var(S) = \frac{n(n-1)(2n+5)}{18}() \tag{13}$$

where x_i and x_j are the variable values of the pixels in years i and j, respectively; n is the length of the time series; and Z obeys a standard normal distribution, with a value ranging from $-\infty$ to $+\infty$. A calculated Z value less than 0 indicates a downward trend, whereas a value greater than 0 indicates an upward trend. For a given significance level ($p < 0.05$), when $|Z| > 1.96$, it passes the significance test at the 0.05 level.

Correlation analysis

In this study, the partial correlation method was used to separate the impact of climate change and human activities on the spatiotemporal changes in the NPP. The effects of human activities and climate change on the spatiotemporal changes in the NPP were examined by controlling climate change and human activities, respectively:

$$R_{xy,z} = \frac{R_{xy} - R_{xz} \times R_{yz}}{\sqrt{\left(1 - R_{xz}^2\right) \times \left(1 - R_{yz}^2\right)}}() \tag{14}$$

where $R_{xy,z}$ is the partial correlation coefficient between x and y, excluding the impact of variable z; x and y are dependent variables; z is the control variable; and R_{xy}, R_{xz}, and R_{yz} are the simple correlation coefficients between x, y, and z. Finally, a bilateral t test was conducted to assess the significance of the partial correlation coefficient, with a significance level of 0.05.

In the regions where climate change controlled the spatiotemporal variation in the NPP, the areas where precipitation, the annual average temperature, and potential evapotranspiration mainly controlled the spatiotemporal variation in the NPP were identified through correlation analysis:

$$R_{xy} = \frac{\sum_{i=1}^{n}(x_i-\bar{x})(y_i-\bar{y})}{\sqrt{\sum_{i=1}^{n}(x_i-\bar{x})^2}\sqrt{\sum_{i=1}^{n}(y_i-\bar{y})^2}}() \tag{15}$$

where R_{xy} is the correlation coefficient between x_i and y_i, which are the NPP and climate factor, respectively, and $\bar{x}$

and $\bar{y}$ are the annual average NPP and mean climate factor, respectively, from 2000 to 2020.

Results

Spatiotemporal characteristics of NPP in Exibei in 2000–2020

The spatial and temporal distributions of the NPP are shown in Fig. 2, which reveals that the NPP demonstrated obvious spatial heterogeneity. However, the annual average NPP exhibited a similar spatial distribution, and the NPP in the region west of Exibei was significantly higher than that in the region east of the study area. The distribution interval of the NPP values was mainly 200–400 g C m^{-2} year^{-1}, accounting for 38.39% of the total area. The high NPP values (over 1000 g C m^{-2} year^{-1}) were observed in 2.22% of the total study area, which were

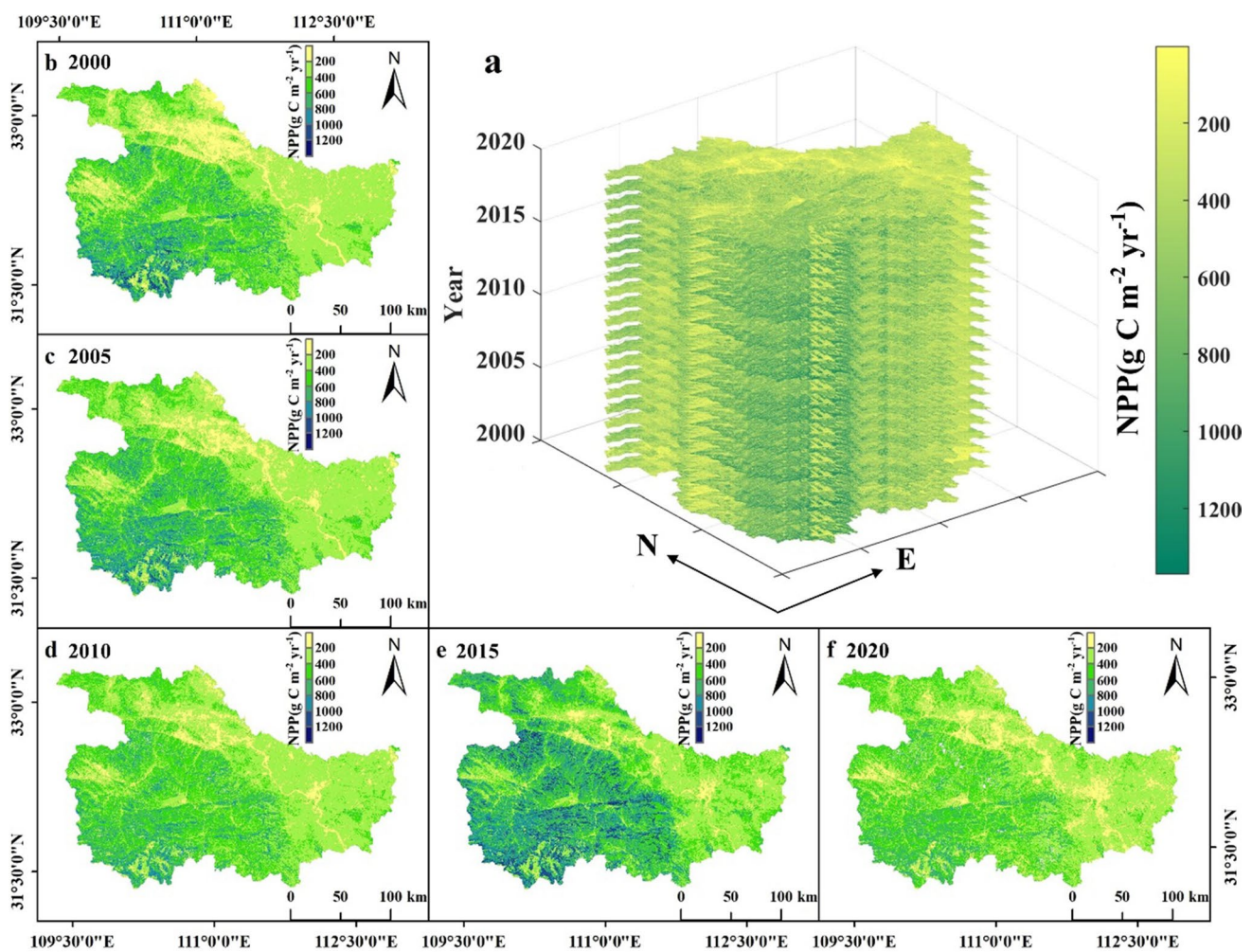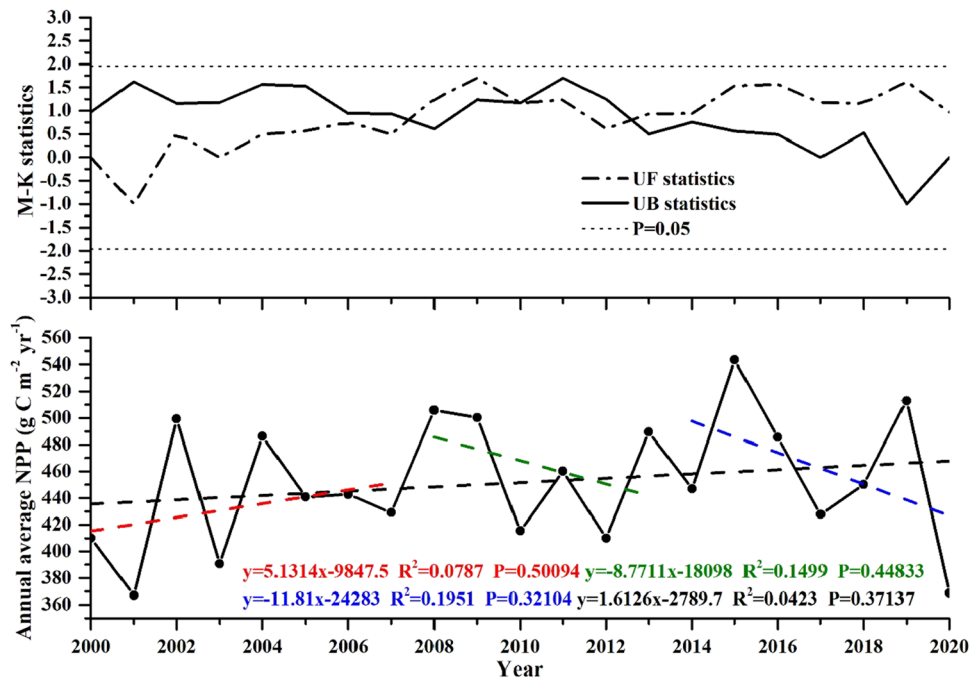**Fig. 2** Spatiotemporal distribution of NPP in Exibei from 2000 to 2020

distributed mainly in Southwest Exibei, and the low NPP values (under 200 g C m^{-2} year^{-1}) covered about 11.29% of the total area, which were mostly scattered from the northwest to the middle western part of Exibei.

From the viewpoint of temporal change, overall, from 2000 to 2020, 61.7% (an area of 28,788 km^2) of the total area of Exibei showed an increasing NPP trend, and the trend that passed the t test ($p < 0.05$) covered 21.4% (an area of 9,986 km^2) of the total area (Fig. 4). The regions with a significant increase in the NPP were distributed mainly north and west of Exibei. The proportion of the NPP with a decreasing trend (34.63%) was far less than that with an increasing trend. The area that demonstrated a significant reduction in the NPP was only 3114 km^2, which accounted for 6.67% of the total area and was concentrated east and southwest of Exibei. Additionally, the areas that showed no change in the NPP accounted for 1.87% (an area of 873 km^2) of the total area of Exibei. The time-series annual average NPP was divided into three phases (i.e., 2000–2007, 2008–2013, and 2014–2020) based on the results of the M–K statistics (Fig. 3). The annual average NPP in 2000–2007 exhibited an increasing trend, whereas that in 2008–2013 and 2014–2020 showed a decreasing trend. The overall trend was on the rise at a low but non-significant annual rate of 1.61 g C m^{-2} year^{-1} in the period of 2000–2020. Moreover, from 2000 to 2020, the annual average NPP in Exibei ranged from 368.52 to 543.54 g C m^{-2} year^{-1}. Overall, (Fig. 4) indicated the regional average NPP in Exibei in the period of 2000–2020 was approximately 451.60 g C m^{-2} year^{-1}, with the highest in 2015 and the lowest in 2020.

Impact of combined effects between climate and HID on NPP change

Table 1 and Fig. 5 reveal the effects of the climate and HID on the significant changes in the NPP in terms of quantity and spatial distribution. The climate, HID, and their combined effects significantly explained 49.13% (passed the t test, $p < 0.05$) of the changes in the NPP in Exibei from 2000 to 2020. At the same time, the effects significantly explained 43.98% and 65.65% (passed the t test, $p < 0.05$) of the increasing and decreasing changes in the NPP in Exibei from 2000 to 2020, respectively.

The changes in the NPP caused significantly by the climate and HID covered 690.13 km^2 and 8593.94 km^2, respectively, which illustrated that the changes in the NPP in Exibei were affected mainly by the HID. At the same time, the areas where the climate and HID together contributed significantly to the changes in the NPP amounted to 882.56 km^2. In the joint action of the climate and HID, the positive effect of the climate was observed mainly in the east, and the negative effect was mainly seen in north of Exibei. Moreover, the combined effects of the climate and HID resulted in a significant increase and decrease in the NPP in an area of 344.44 km^2 and 249.25 km^2, respectively. In the interaction of the climate and HID, the climate mainly played a positive role, whereas the HID played a negative role.

Impact of HID on NPP change

The areas that exhibited a significant positive correlation between HID and NPP changes were mainly distributed

Fig. 3 Interannual change in annual average NPP in Exibei from 2000 to 2020 (The above figure is the M–K trend test chart, and the following figure is the fitting chart of NPP change trend in different time periods)

Fig. 4 Spatiotemporal changes in NPP in Exibei from 2000 to 2020 (The small image shows the proportion of areas with different change trends of NPP. **a**, **b** represents $p < 0.05$ and no significant, respectively)
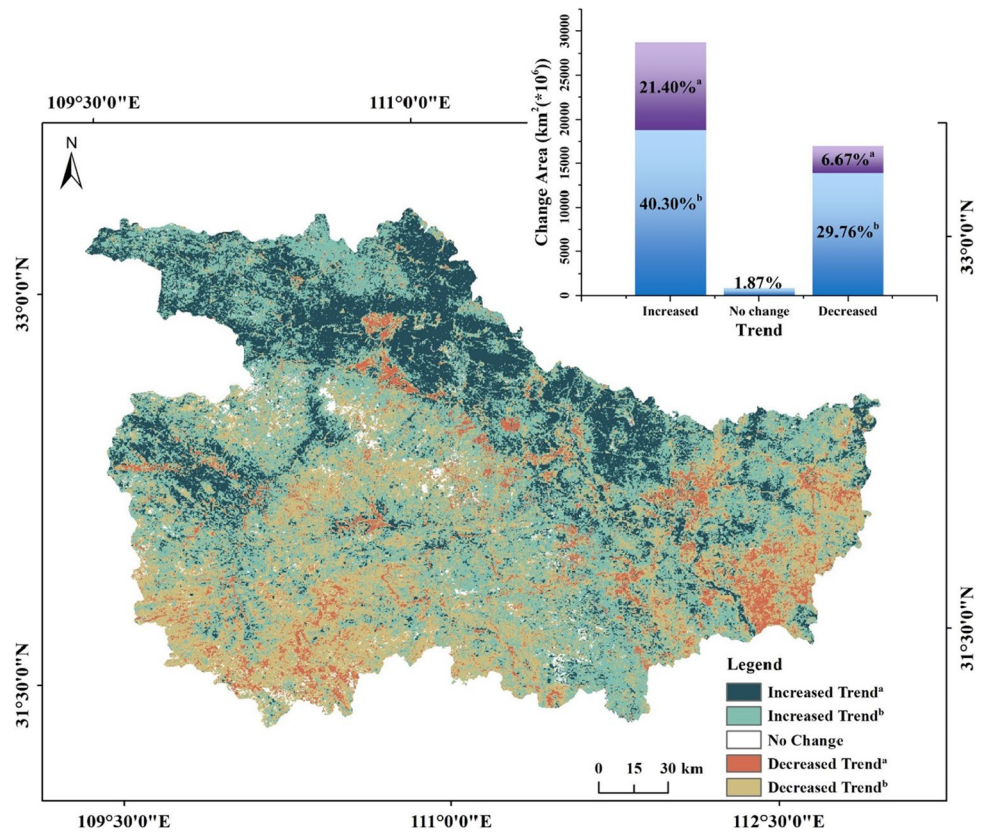

Impact of different climate factors on NPP change

The areas where the climate had a significant positive effect on the NPP changes were located in the east and southwest of Exibei (Fig. 5). And the areas where the climate had a significant negative effect were located in the center of Exibei. In terms of quantity, only 32.63 km² and 75.88 km² of the area that demonstrated significantly increasing and decreasing changes in the NPP were significantly related to the climate, respectively (Table 1).

The spatial patterns of the correlations between the NPP and temperature, precipitation, and potential evapotranspiration during the study period were further analyzed. According to Fig. 6a and b, among the climate factors significantly related to the changes in the NPP, potential evapotranspiration covered an area of 434.40 km², which indicated that it played a dominant role. Potential evapotranspiration was significantly negatively correlated with the NPP in the area southeast of Exibei. As shown in Fig. 6d, the increase in the potential evapotranspiration led to a significant decrease in the NPP in the area southeast of Exibei. Figure 6a and c illustrate that the significant changes in the NPP caused by temperature covered an area of 152.69 km². Thus, temperature was positively correlated with the significant changes in the NPP, thereby indicating that the increase in the temperature contributed to the increase in the NPP, but the

Table 1 NPP change areas caused by climate and human activities

| Region Factors	Whole study area (km²)	significant increase of NPP (km²)	significant decrease of NPP (km²)
Climate	690.13	32.63	75.88
HID	8593.94	4015.25	1719.06
Climate + HID	882.56	344.44	249.25

in the north of Exibei, and the areas that showed a significant negative correlation were mainly distributed in the central of Exibei (Fig. 5). On the other hand, the areas that exhibited a significantly increasing change in the NPP significantly related to HID amounted to 4015.25 km² (Table 1), which were mainly distributed in the middle east of Exibei, with significant positive effects. And, the significant negative effects in north and west. The significantly decreasing changes in the NPP caused by the HID were observed in an area of 1719.06 km². The significant negative correlation between the HID and NPP, with a significantly decreasing trend, was mainly seen in the center of the study area, whereas the positive correlation exhibited a sporadic distribution.

Fig. 5 Spatial patterns of partial correlations between NPP and climate and HID in 2000–2020. (**A**, **B**, and **C** are the significant effects of the climate and HID on the NPP changes, the significant effects of the climate and HID on the significantly increasing NPP, and the significant effects of the climate and HID on the significantly decreasing NPP, respectively; **A**(a) is the significant impact of the climate and HID on the NPP changes; **A**(b) is the significant effect of the climate on the NPP changes in the combined effects of the climate and HID on the NPP changes; **A**(c) is the significant effect of the HID on the NPP changes in the combined effects of the climate and HID on the NPP changes; **B**(a) is the significant impact of the climate and HID on the significantly increasing NPP; **B**(b) is the significant effect of the climate on the significantly increasing NPP in the combined effects of the climate and HID on the significantly increasing NPP; **B**(c) is the significant effect of the HID on the significantly increasing NPP in the combined effects of the climate and HID on the significantly increasing NPP; **C**(a) is the significant impact of the climate and HID on the significantly decreasing NPP; **C**(b) is the significant effects of the climate on the significantly decreasing NPP in the combined effects of the climate and HID on the significantly decreasing NPP; **C**(c) is the significant effect of the HID on the significantly decreasing NPP in the combined effects of the climate and HID on the significantly decreasing NPP)
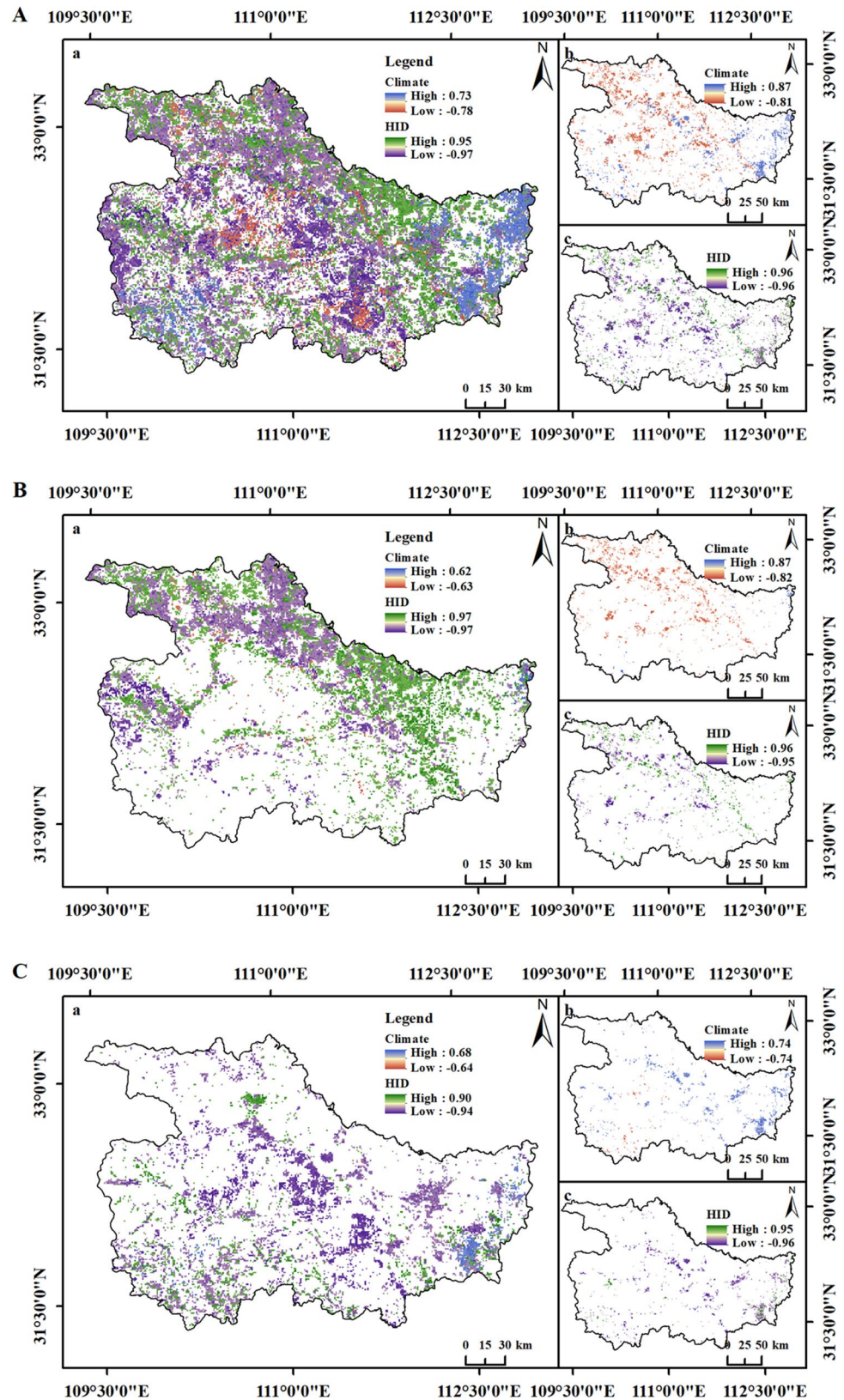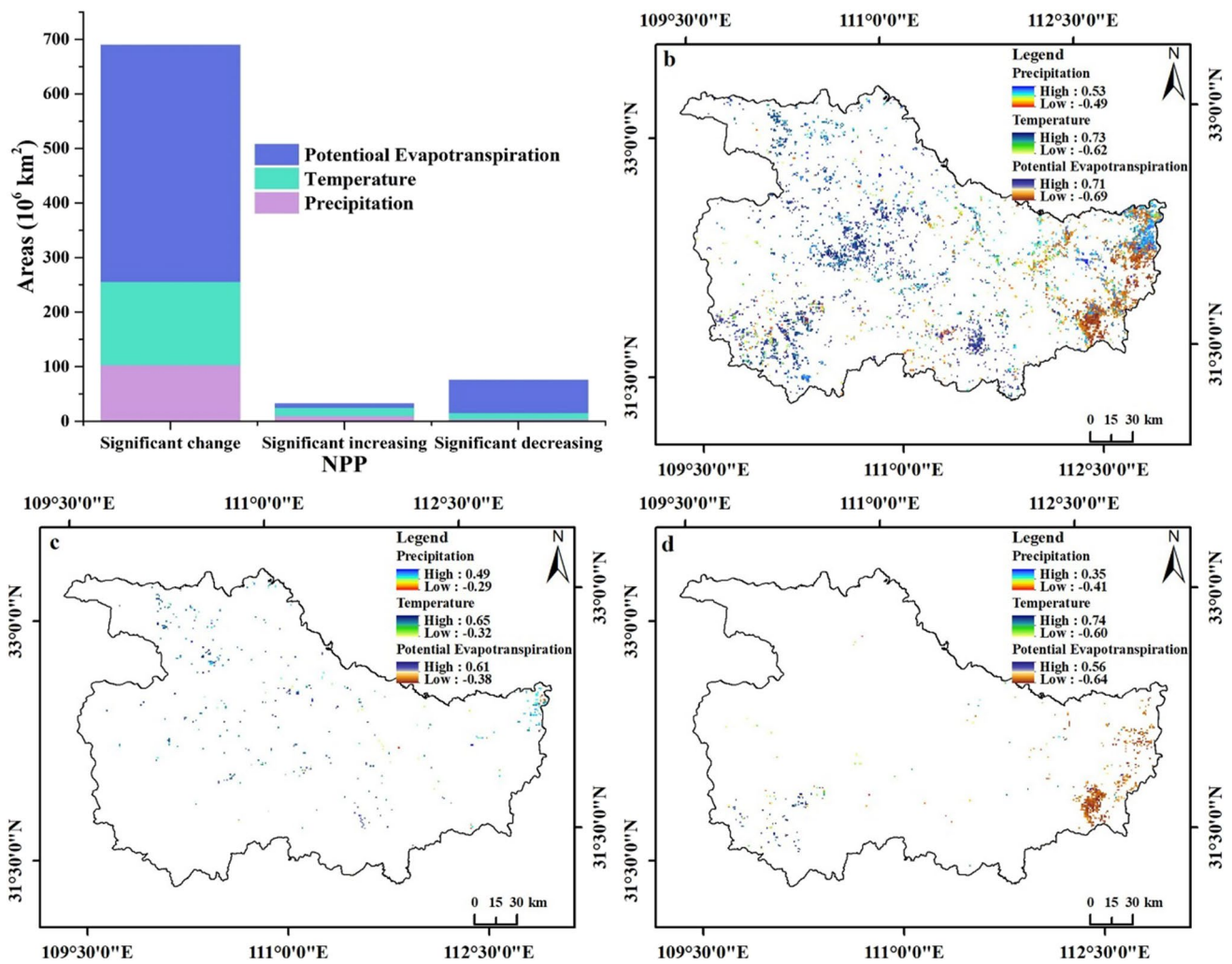
Fig. 6 Spatial patterns of effect of climate on NPP in Exibei in 2000–2020 (**a** is the area with NPP changes caused by the climate, with significant changes, significant increased changes, and significant decreased changes; **b** is the spatial pattern of the effect of the climate on the NPP in the significant change area; **c** is the spatial pattern of the effect of the climate on the NPP in the significant increased change area; **d** is the spatial pattern of the effect of the climate on the NPP in the significant decreased change area)

distribution was scattered in different areas. According to Fig. 6a and c, the contribution of precipitation to the significant changes in the NPP covered an area of 103.04 km^2, and the increase in the NPP east of Exibei was caused by the increase in the precipitation.

Discussion

The temporal trend characteristics of NPP, climate, and HID in three time periods

Overall, a slight increasing trend was observed in the potential evapotranspiration, temperature, and HID in Exibei in the period of 2000–2020, which was similar to the trend of the NPP. The slight increasing trend of the NPP in Exibei

observed in this study is consistent with that observed by Wu et al. (2022). However, precipitation decreased slightly. Specifically, the interannual fluctuations of the NPP, potential evapotranspiration, temperature, and HID, were substantial. According to the fluctuation trend of the NPP, the NPP showed an increasing trend in the period of 2000–2007, which was the same as the trend of temperature and potential evapotranspiration and opposite that of precipitation and the HID. In the period of 2008–2013 and 2014–2020, the NPP showed a decreasing trend. Specifically, the NPP change trend in the former period was the same as that of precipitation and temperature but opposite that of potential evapotranspiration and the HID. Meanwhile, the NPP change trend in the latter period was the same as that of precipitation but opposite that of temperature, potential evapotranspiration, and the HID. Therefore, according to

the temporal change trends (Fig. 7), a negative correlation existed between the NPP and HID. Nevertheless, the climate change trends could not explain the NPP change trends, mainly because the effects of the climate on the NPP were spatially heterogeneous.

Spatial heterogeneity of effects of climate and HID on NPP

From 2000 to 2020, the spatial heterogeneity of the NPP changes in Exibei was obvious. The significant increase in the NPP was distributed mainly in the area north of Exibei, and the distribution of the significant decrease was scattered but mostly concentrated in the central and eastern parts of Exibei. Although the forest land in Exibei accounts for over 60%, while the cultivated land is around 30%, according to the partial correlation analysis between the NPP and climate and HID, the areas where the HID significantly affected the NPP changes amounted to 8593.94 km^2, which is much larger than the area of 690.13 km^2 affected by the climate. The above results indicated that compared with forests significantly affected by climate, human activities had a more

significant impact on the NPP change of cultivated land in Exibei. Of course, the impact mechanisms of human activities on NPP changes in cultivated land under different natural environments were different. Specifically, in the areas with a significant increase in the NPP, the significant correlation between the HID and NPP was mainly within the range of cultivated land, because human activities have no significant impact on vegetation far from human settlements (FAO, UN 2020). The HID had a significant positive correlation with the significantly increasing NPP, which was distributed in the area in the middle east of Exibei. As the area was flat, developed agriculture and the cultivation of farmland would increase the crop production. In Northern Exibei, the HID had a significant negative correlation with the significantly increasing NPP, which was due to the high terrain and low agricultural production in the region and perhaps to the implementation of the policy of the Grain for Green Program and reduced human activities within the forestland (Ge et al. 2021). Previous studies showed that the impact of human activities on the NPP was more pronounced on the horizontal scale than on the vertical scale of the terrain (Yin et al. 2020). In the areas that demonstrated
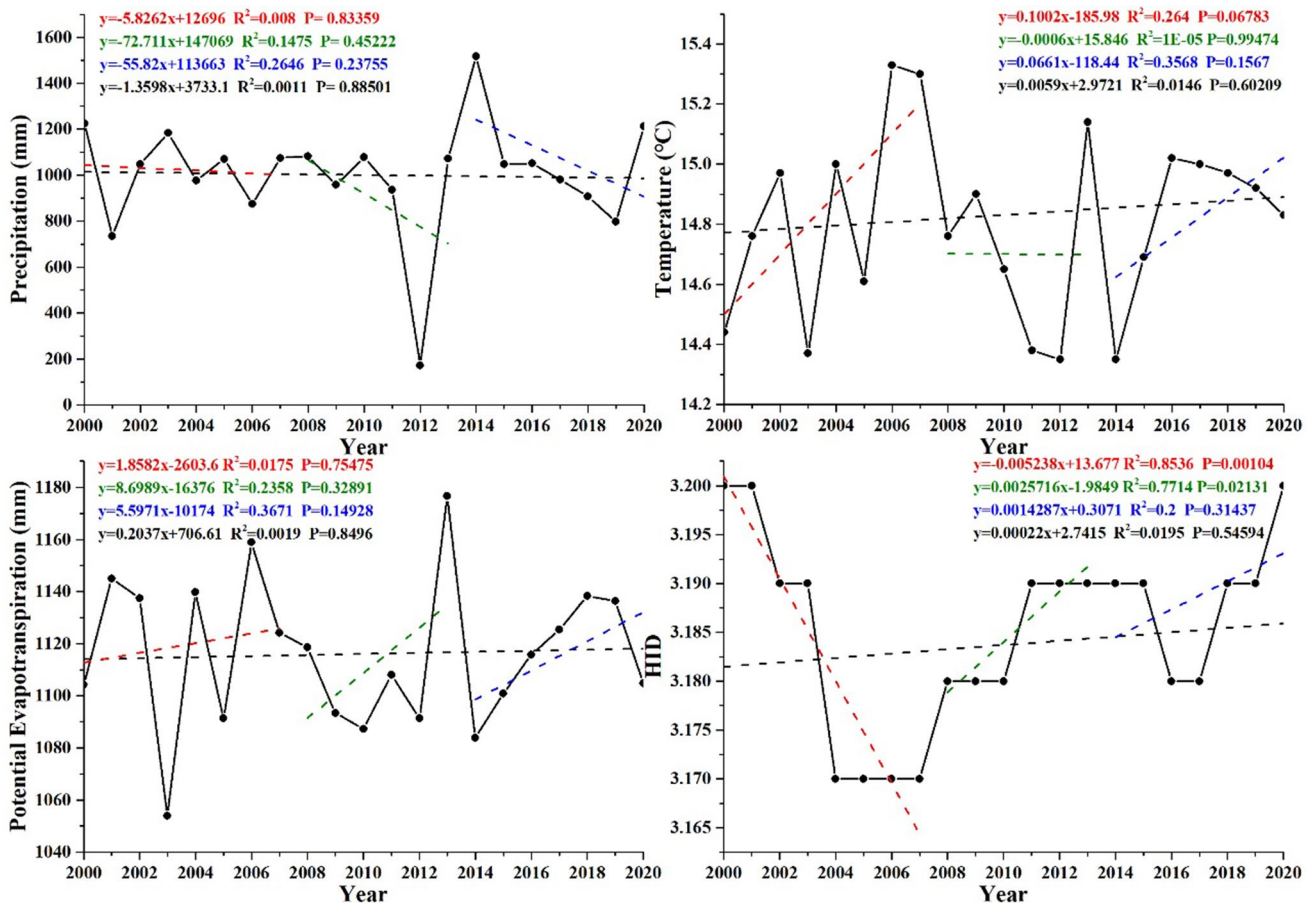

Fig. 7 Interannual changes in climate factors and HID

a significant decrease in the NPP, the significant correlation between the HID and NPP was mainly within the range of the rural–urban land and shrubs. The HID had a significant negative correlation with the significantly decreasing NPP, which was located in Central Exibei. On the one hand, the expansion of the rural–urban land utilized a large amount of the cultivated land resources. On the other hand, the expansion was due to the change of the broad-leaved forest to shrubs.

Previous studies indicated that ecosystems in arid and semiarid regions are highly sensitive to climate change (Zhang and Ren 2017). Exibei is located in the humid region of China, with a single climatic zone. Therefore, the changes in the NPP in Exibei were less affected by the climate than other factors. However, potential evapotranspiration played a relatively important role in the NPP changes, especially in the southeastern part of Exibei, where potential evapotranspiration was negatively correlated with the significant decrease in the NPP. This outcome was observed, because shrubs and rural–urban land occupied the cultivated land, resulting in a decrease in vegetation coverage and an increase in the potential evapotranspiration. In addition, the areas that exhibited a significant increase in the NPP were positively correlated with precipitation and temperature. Increasing temperatures can prolong the growth period of plants and promote plant productivity (Lian et al. 2020; Piao et al. 2007). However, forestland in humid regions is less sensitive to precipitation, so the NPP changes in the forestland due to precipitation were minimal.

Methodological uncertainties and limitations

The impact of human activities on vegetation often has a lag effect. Therefore, the time nodes affected by human activities should be considered in future research. In addition, this study separated the effects of the climate and human activities on NPP changes through partial correlation analysis but did not deeply examine the combined effects of the climate and human activities on NPP changes. This study did not laterally compare different methods for separating the effects of the climate and human activities on NPP, such as machine learning (Leroux et al. 2017; Shi et al. 2020).

Conclusion

From 2000 to 2020, NPP, with an increasing trend, was observed in an area of 28,788 km^2 (61.7%) in Northwest Hubei, of which the area that demonstrated a significant increase was 9986 km^2 (21.4%) and distributed mainly in the northern part of the study area. The size of the area with a decreasing NPP trend was 16,999 km^2 (36.43%), of which the area that exhibited a significant decrease was 3114 km^2

(6.67%) and distributed mainly southwest and southeast of the study area.

The climate and human activities explained the NPP changes in an area of 690.13 km^2 and 8593.94 km^2, respectively, thereby indicating that from 2000 to 2020, the changes in the NPP in Northwest Hubei were mainly from human activities. The impact of the climate and human activities on the NPP demonstrated obvious spatial heterogeneity. The farming of cultivated land in the central eastern region led to a significant increase in the NPP. However, in the northwestern region, with a high terrain and little human activity, NPP also increased significantly. The expansion of the rural–urban land and change of the broad-leaved forest to shrubs resulted in a significant decrease in the NPP in the central region. The changes in the NPP east of Northwest Hubei were mainly from the climate. Owing to the occupation of cultivated land by shrubs and rural–urban land, vegetation coverage decreased, the potential evapotranspiration increased, and the NPP decreased significantly.

Author contribution Shuai Shao: collected, analyzed and interpreted the data and results. Meanwhile, Shuai Shao wrote the manuscript. Yong Yang: designed and directed the experimental scheme and writing. All authors read and approved the final manuscript.

Data availability The datasets generated during and/or analyzed during the current study are available from the corresponding author on reasonable request.

Declarations

Ethics approval Not applicable.

Consent to participate Not applicable.

Consent for publication All authors have read the manuscript and agreed to publish the manuscript.

Conflict of interest The authors declare no competing interests.

References

Bai XY, Zhang SR, Li CJ, Xiong L, Song FJ, Du CC, Li MH, Luo Q, Xue YY, Wang SJ (2023) A carbon-neutrality-capactiy index for evaluating carbon sink contributions. Environ Sci Ecotech 15:100237. https://doi.org/10.1016/j.ese.2023.100237

Beltrán-Sanz N, Raggio J, Gonzalez S, Dal Grande F, Prost S, Green A, Pintado A, Sancho LG (2022) Climate change leads to higher NPP at the end of the century in the Antarctic Tundra: response patterns through the lens of lichens. Sci Total Environ 835:155495

Bejagam V, Sharma A (2022) Impact of climatic changes and anthropogenic activities on ecosystem net primary productivity in India

19842

Environmental Science and Pollution Research (2024) 31:19831–19843

during 2001–2019. Ecol Inform 70 https://doi.org/10.1016/j.eco-inf.2022.101732

Chen T, Bao AM, Jiapaer G, Guo H, Zheng GX, Jiang LL, Chang C, Tuerhanjiang L (2019) Disentangling the relative impacts of climate change and human activities on arid and semiarid grasslands in Central Asia during 1982–2015. Sci Total Environ 653:1311–1325

Dariane AB, Pouryafar E (2021) Quantifying and projection of the relative impacts of climate change and direct human activities on streamflow fluctuations. Clim Change 165:34. https://doi.org/10.1007/s10584-021-03060-w

FAO UN (2020) The state of the world's forests: forests, biodiversity and people. Food and agriculture organization rome, In

Field CB, Randerson JT, Malmstrom CM (1995) Global net primary production - combining ecology and remote-sensing. Remote Sens Environ 51:74–88

Friedlingstein P, Jones MW, O'Sullivan M, Andrew RM, Hauck J, Peters GP, Peters W, Pongratz J, Sitch S, Le Quere C, Bakker DCE, Canadell JG, Ciais P, Jackson RB, Anthoni P, Barbero L, Bastos A, Bastrikov V, Becker M, Bopp L, Buitenhuis E, Chandra N, Chevallier F, Chini LP, Currie KI, Feely RA, Gehlen M, Gilfillan D, Gkritzalis T, Goll DS, Gruber N, Gutekunst S, Harris I, Haverd V, Houghton RA, Hurtt G, Ilyina T, Jain AK, Joetzjer E, Kaplan JO, Kato E, Goldewijk KK, Korsbakken JI, Landschutzer P, Lauvset SK, Lefevre N, Lenton A, Lienert S, Lombardozzi D, Marland G, McGuire PC, Melton JR, Metzl N, Munro DR, Nabel JEMS, Nakaoka SI, Neill C, Omar AM, Ono T, Peregon A, Pierrot D, Poulter B, Rehder G, Resplandy L, Robertson E, Rodenbeck C, Seferian R, Schwinger J, Smith N, Tans PP, Tian HQ, Tilbrook B, Tubiello FN, van der Werf GR, Wiltshire AJ, Zaehle S (2019) Global carbon budget 2019. Earth Syst Sci Data 11:1783–1838

Ge WY, Deng LQ, Wang F, Han JQ (2021) Quantifying the contributions of human activities and climate change to vegetation net primary productivity dynamics in China from 2001 to 2016. Sci Total Environ 773:145648. https://doi.org/10.1016/j.scitotenv.2021.145648

Haberl H (1997) Human appropriation of net primary production as an environmental indicator: Implications for sustainable development. Ambio 26:143–146

Haberl H, Plutzar C, Erb KH, Gaube V, Pollheimer M, Schulz NB (2005) Human appropriation of net primary production as determinant of avifauna diversity in Austria. Agric Ecosyst Environ 110:119–131

Hsu JS, Powell J, Adler PB (2012) Sensitivity of mean annual primary production to precipitation. Glob Chang Biol 18:2246–2255

Izaurralde RC, Thomson AM, Rosenberg NJ, Brown RA (2005) Climate change impacts for the conterminous USA: an integrated assessment - Part 6. Distribution and productivity of unmanaged ecosystems. Clim Chang 69:107–126

Kendall MG (1938) A new measure of rank correlation. Biometrika 30:81–93

Koju UA, Zhang JH, Maharjan S, Bai Y, Zhang S, Yao FM (2020) Analysis of spatiotemporal dynamics of forest net primary productivity of Nepal during 2000–2015. Int J Remote Sens 41:4336–4364

Le Quere C, Andrew RM, Friedlingstein P, Sitch S, Hauck J, Pongratz J, Pickers PA, Korsbakken JI, Peters GP, Canadell JG, Arneth A, Arora VK, Barbero L, Bastos A, Bopp L, Chevallier F, Chini LP, Ciais P, Doney SC, Gkritzalis T, Goll DS, Harris I, Haverd V, Hoffman FM, Hoppema M, Houghton RA, Hurtt G, Ilyina T, Jain AK, Johannessen T, Jones CD, Kato E, Keeling RF, Goldewijk KK, Landschutzer P, Lefevre N, Lienert S, Liu Z, Lombardozzi D, Metzl N, Munro DR, Nabel JEMS, Nakaoka S, Neill C, Olsen A, Ono T, Patra P, Peregon A, Peters W, Peylin P, Pfeil B, Pierrot D, Poulter B, Rehder G, Resplandy L, Robertson E, Rocher M, Rodenbeck C, Schuster U, Schwinger J, Seferian R, Skjelvan I,

Steinhoff T, Sutton A, Tans PP, Tian HQ, Tilbrook B, Tubiello FN, van der Laan-Luijkx IT, van der Werf GR, Viovy N, Walker AP, Wiltshire AJ, Wright R, Zaehle S, Zheng B (2018) Global carbon budget 2018. Earth Syst Sci Data 10:2141–2194

Leroux L, Begue A, Lo Seen D, Jolivot A, Kayitakire F (2017) Driving forces of recent vegetation changes in the Sahel: lessons learned from regional and local level analyses. Remote Sens Environ 191:38–54

Li CH, Wang YT, Wu XD, Cao HJ, Li WP, Wu TH (2021) Reducing human activity promotes environmental restoration in arid and semi-arid regions: a case study in Northwest China. Sci Total Environ 768:144525. https://doi.org/10.1016/j.scitotenv.2020.144525

Lian X, Piao SL, Li LZX, Li Y, Huntingford C, Ciais P, Cescatti A, Janssens IA, Penuelas J, Buermann W, Chen AP, Li XY, Myneni RB, Wang XH, Wang YL, Yang YT, Zeng ZZ, Zhang YQ, McVicar TR (2020) Summer soil drying exacerbated by earlier spring greening of northern vegetation. Sci Adv 6:eaax0255. https://doi.org/10.1080/15481603.2023.2286744

Li S, He S (2022) The variation of net primary productivity and underlying mechanisms vary under different drought stress in Central Asia from 1990 to 2020. Agric for Meteorol 314:108767

Liu YY, Wang Q, Zhang ZY, Tong LJ, Wang ZQ, Li JL (2019) Grassland dynamics in responses to climate variation and human activities in China from 2000 to 2013. Sci Total Environ 690:27–39

Los SO (1998) Linkages between global vegetation and climate: an analysis based on NOAA advanced very high resolution radiometer data. PhD dissertation. National Aeronautics and Space Administration (NASA)

Mann HB (1945) Nonparametric tests against trend. Econometrica 13:245–259

Nayak RK, Patel NR, Dadhwal VK (2013) Inter-annual variability and climate control of terrestrial net primary productivity over India. Int J Climatol 33:132–142

Pettorelli N, Chauvenet ALM, Duffy JP, Cornforth WA, Meillere A, Baillie JEM (2012) Tracking the effect of climate change on ecosystem functioning using protected areas: Africa as a case study. Ecol Indic 20:269–276

Piao SL, Friedlingstein P, Ciais P, Viovy N, Demarty J (2007) Growing season extension and its impact on terrestrial carbon cycle in the Northern Hemisphere over the past 2 decades. Global Biogeochem Cy 21 https://doi.org/10.1029/2006GB002888

Potter CS, Randerson JT, Field CB, Matson PA, Vitousek PM, Mooney HA, Klooster SA (1993) Terrestrial ecosystem production - a process model-based on global satellite and surface data. Global Biogeochem Cy 7:811–841

Qi XZ, Jia JH, Liu HY, Lin ZS (2019) Relative importance of climate change and human activities for vegetation changes on China's silk road economic belt over multiple timescales. CATENA 180:224–237

Ruimy A, Saugier B, Dedieu G (1994) Methodology for the estimation of terrestrial net primary production from remotely sensed data. J Geophys Res-Atmos 99:5263–5283

Shi Y, Jin N, Ma XL, Wu BY, He QS, Yue C, Yu Q (2020) Attribution of climate and human activities to vegetation change in China using machine learning techniques. Agric For Meteorol 294:108146. https://doi.org/10.1016/j.agrformet.2020.108146

Sokal RR (1982) Citation classic - biometry - the principles and practice of statistics in biological-research. Current Contents/Agric Biol Environ Sci 22–22

Stevens-Rumann CS, Kemp KB, Higuera PE, Harvey BJ, Rother MT, Donato DC, Morgan P, Veblen TT (2018) Evidence for declining forest resilience to wildfires under climate change. Ecol Lett 21:243–252

Teng MJ, Zeng LX, Hu WJ, Wang PC, Yan ZG, He W, Zhang Y, Huang ZL, Xiao WF (2020) The impacts of climate changes and human

activities on net primary productivity vary across an ecotone zone in Northwest China. Sci Total Environ 714:136691. https://doi.org/10.1016/j.scitotenv.2020.136691

Wang ZY, Zhong JL, Lan H, Wang ZB, Sha ZY (2019) Association analysis between spatiotemporal variation of net primary productivity and its driving factors in Inner Mongolia, China during 1994–2013. Ecol Indic 105:355–364

Wu LH, Wang SJ, Bai XY, Tian YC, Luo GJ, Wang JF, Li Q, Chen F, Deng YH, Yang YJ, Hu ZY (2020) Climate change weakens the positive effect of human activities on karst vegetation productivity restoration in southern China. Ecol Indic 115:106392. https://doi.org/10.1016/j.ecolind.2020.106392

Wu LZ, Ma XF, Dou X, Zhu JT, Zhao CY (2021) Impacts of climate change on vegetation phenology and net primary productivity in arid Central Asia. Sci Total Environ 796:149055. https://doi.org/10.1016/j.scitotenv.2021.149055

Wu K, Zhou CF, Zhang YX, Xu Y (2022) Long-term spatiotemporal variation of net primary productivity and its correlation with the urbanization: a case study in Hubei Province, China. Front Environ Sci 9:808401. https://doi.org/10.3389/fenvs.2021.808401

Xiao BQ, Bai XY, Zhao CW, Tan Q, Li YB, Luo GJ, Wu LH, Chen F, Li CJ, Ran C, Luo XL, Xi HP, Chen H, Zhang SR, Liu M, Gong SH, Xiong L, Song FJ, Du CC (2023) Responses of carbon and water use efficiencies to climate and land use changes in China's karst areas. J. Hydrol 617 https://doi.org/10.1016/j.jhydrol.2022.128968

Yang HF, Mu SJ, Li JL (2014) Effects of ecological restoration projects on land use and land cover change and its influences on territorial NPP in Xinjiang, China. CATENA 115:85–95

Zhang C, Ren W (2017) Complex climatic and CO2 controls on net primary productivity of temperate dryland ecosystems over central Asia during 1980–2014. J Geophys Res-Biogeo 122:2356–2374

Yang HF, Zhong XN, Deng SQ, Xu H (2021) Assessment of the impact of LUCC on NPP and its influencing factors in the Yangtze River basin, China. Catena 206 https://doi.org/10.1016/j.catena.2021.105542

Zhuang Q, Shao Z, Li D, Huang X, Cai B, Altan O, Wu S (2022) Unequal weakening of urbanization and soil salinization on vegetation production capacity. Geoderma 411:115712

Yin L, Dai EF, Zheng D, Wang YH, Ma L, Tong M (2020) What drives the vegetation dynamics in the Hengduan Mountain region, southwest China: Climate change or human activity? Ecol Indic 112:106013. https://doi.org/10.1016/j.ecolind.2019.106013

Zhang YZ, Wang Q, Wang ZQ, Yang Y, Li JL (2020) Impact of human activities and climate change on the grassland dynamics under different regime policies in the Mongolian Plateau. Sci Total Environ 698:134304. https://doi.org/10.1016/j.scitotenv.2019.134304

Zhang YL, Song CH, Hwang T, Novick K, Coulston JW, Vose J, Dannenberg MP, Hakkenberg CR, Mao JF, Woodcock CE (2021) Land cover change-induced decline in terrestrial gross primary production over the conterminous United States from 2001 to 2016. Agric For Meteorol 308:108609. https://doi.org/10.1016/j.agrformet.2021.108609